# Small-molecule inhibition of 6-phosphofructo-2-kinase activity suppresses glycolytic flux and tumor growth

**Brian Clem,[1,3] Sucheta Telang,[1,3] Amy Clem,[1,3] Abdullah Yalcin,[1,2,3] Jason Meier,[2] Alan Simmons,[1,3] Mary Ann Rasku,[1,3] Sengodagounder Arumugam,[1,3] William L. Dean,[2,3] John Eaton,[1,3] Andrew Lane,[1,3] John O. Trent,[1,2,3] and Jason Chesney[1,2,3]**

Departments of [1]Medicine and [2]Biochemistry and Molecular Biology and [3]Molecular Targets Group, James Graham Brown Cancer Center, University of Louisville, Louisville, Kentucky

## Abstract

**6-Phosphofructo-1-kinase, a rate-limiting enzyme of glycolysis, is activated in neoplastic cells by fructose-2,6-bisphosphate (Fru-2,6-BP), a product of four 6-phosphofructo-2-kinase/fructose-2,6-bisphosphatase isozymes (PFKFB1-4). The inducible PFKFB3 isozyme is constitutively expressed by neoplastic cells and required for the high glycolytic rate and anchorage-independent growth of *ras*-transformed cells. We report herein the computational identification of a small-molecule inhibitor of PFKFB3, 3-(3-pyridinyl)-1-(4-pyridinyl)-2-propen-1-one (3PO), which suppresses glycolytic flux and is cytostatic to neoplastic cells. 3PO inhibits recombinant PFKFB3 activity, suppresses glucose uptake, and decreases the intracellular concentration of Fru-2,6-BP, lactate, ATP, $NAD^+$, and NADH. 3PO markedly attenuates the proliferation of several human malignant hematopoietic and adenocarcinoma cell lines ($IC_{50}$, 1.4-24 μmol/L) and is selectively cytostatic to *ras*-transformed human bronchial epithelial cells relative to normal human bronchial epithelial cells. The PFKFB3 enzyme is an essential molecular target of 3PO because transformed cells are rendered resistant to 3PO by ectopic expression of PFKFB3 and sensitive to 3PO by heterozygotic genomic deletion of PFKFB3. Importantly, i.p. administration of 3PO (0.07 mg/g) to tumor-bearing mice markedly reduces the intracellular concentration of Fru-2,6-BP, glucose uptake, and growth of established tumors *in vivo*. Taken together, these data support the clinical development of 3PO and other PFKFB3 inhibitors as chemotherapeutic agents. [Mol Cancer Ther 2008;7(1):110–20]**

## Introduction

Neoplastic transformation causes a marked increase in glucose uptake and catabolic conversion to lactate, which forms the basis for the most specific cancer diagnostic examination—positron emission tomography of 2-$^{18}$F-fluoro-2-deoxyglucose ($^{18}$F-2-DG) uptake (1). The protein products of several oncogenes directly increase glycolytic flux even under normoxic conditions, a phenomenon originally termed the Warburg effect (2, 3). For example, c-*myc* is a transcription factor that promotes the expression of glycolytic enzyme mRNAs, and its expression is increased in several human cancers regardless of the oxygen pressure (4, 5). Understanding the precise effectors of common oncogenes that regulate the metabolic shifts required for neoplastic growth and survival should introduce a plethora of metabolic targets for the development of antineoplastic agents.

Recently, the *ras* signaling pathway has been invoked as a central regulator of the glycolytic phenotype of cancer (6–9). Stable transfection of an oncogenic allele of H-*ras* into immortalized cells increases glucose uptake, lactate secretion, and sensitivity to glycolytic inhibitors (8, 10, 11). Oncogenic *ras* signaling causes the activation of 6-phosphofructo-1-kinase (PFK-1), the first irreversible and committed step of glycolysis (10). The increase in the activity of PFK-1 by *ras* is due in part to an increase in the steady-state concentration of a potent PFK-1 allosteric activator, fructose-2,6-bisphosphate (Fru-2,6-BP; Fig. 1; ref. 10). Fru-2,6-BP relieves the tonic allosteric inhibition of PFK-1 caused by ATP, allowing untethered glycolytic flux through the PFK-1 checkpoint and into anabolic pathways required for growth (12). That *ras* increases Fru-2,6-BP in immortalized cells to increase glycolytic flux indicates that this particular metabolic regulatory pathway may be essential for neoplastic transformation.

The steady-state concentration of Fru-2,6-BP is controlled by a family of bifunctional 6-phosphofructo-2-kinase/fructose-2,6-bisphosphatases (PFK-2/FBPases), which are encoded by four genes *PFKFB1-4* (13). An inducible isoform of PFK-2/FBPase encoded by the *PFKFB3* gene (termed the PFKFB3 isozyme; initially reported as iPFK2, placental PFK2, ubiquitous PFK2, and PGR1; refs. 14–17) is up-regulated by inflammatory and hypoxic stimuli and contains an oncogene-like AU-rich element in the 3′-untranslated region (14, 18). The PFKFB3 isozyme is overexpressed by leukemias as well as by colon, prostate,

Received 7/18/07; revised 10/5/07; accepted 11/19/07.

**Grant support:** Department of Defense Breast Cancer Research Program Postdoctoral Multidisciplinary Award BC051684 (B. Clem), Leukemia and Lymphoma Society Translational Research Grant (J. Chesney), NIH grant 1 R01 CA11642801 (J. Chesney), Philip Morris External Research Program (unrestricted; J. Chesney), and NIH grant 1P20 RR18733 (JC and J.O. Trent).

The costs of publication of this article were defrayed in part by the payment of page charges. This article must therefore be hereby marked *advertisement* in accordance with 18 U.S.C. Section 1734 solely to indicate this fact.

**Requests for reprints:** Jason Chesney, Room 204E, Delia Baxter II Building, 580 South Preston Street, Louisville, KY 40202. Phone: 502-852-3679. E-mail: jason.chesney@louisville.edu



doi:10.1158/1535-7163.MCT-07-0482

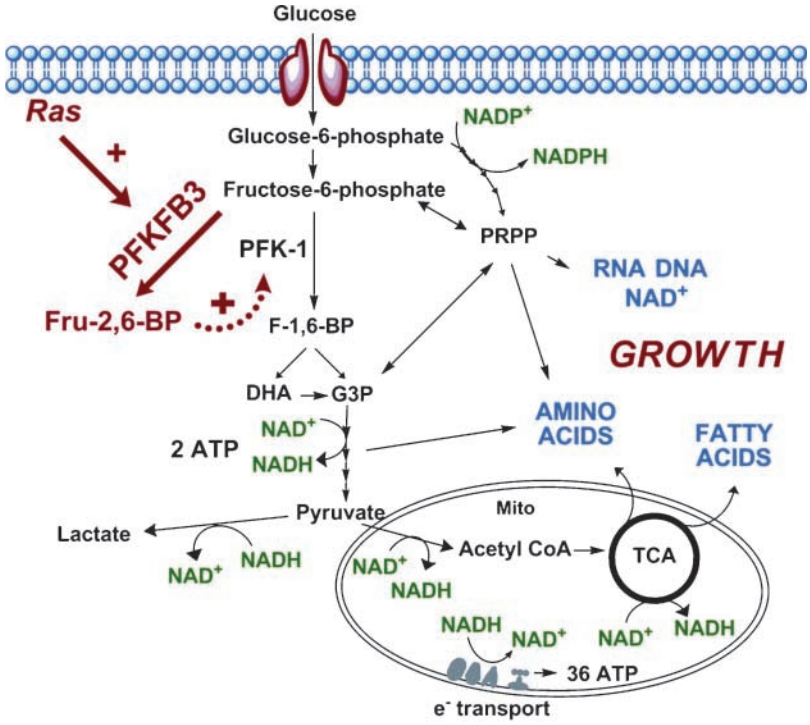


**Figure 1.** PFKFB3 produces Fru-2,6-BP, a potent stimulator of glycolysis. Oncogenic *ras* increases the expression and activity of PFKFB3, which produces Fru-2,6-BP, an allosteric activator of PFK-1. High PFK-1 activity causes increased glycolytic flux, allowing for the increased production of the macromolecules (RNA, DNA, amino acids, fatty acids, etc.) and energy (NADH and ATP) necessary for enhanced cellular proliferation. Because glycolysis, the tricarboxylic acid cycle and electron transport are tightly coupled through $NAD^+$/NADH, disruption of any of these pathways will result in diminished anabolism and energy production, ultimately leading to suppression of growth. *F-1,6-BP,* fructose-1,6-bisphosphate; *DHA,* dihydroxyacetone; *G3P,* glyceraldehyde-3-phosphate; *PRPP,* 5-phospho-D-ribosyl-1-pyrophosphate.

lung, breast, pancreas, thyroid, and ovarian tumors and is required for the growth of certain leukemia and cervical cancer cell lines (14, 19, 20). Taken together, these observations indicate that among the family of four PFK-2/FBPases, the PFKFB3 isozyme may prove to be an important metabolic effector supporting neoplastic transformation.

The expression of the PFKFB3 isozyme was recently observed to be increased on immortalization and transformation of normal human bronchial epithelial (NHBE) cells (21). In addition, heterozygous $PFKFB3^{+/-}$ mouse fibroblasts immortalized and transformed with large T antigen and H-$ras^{V12}$ maintain a reduced intracellular concentration of Fru-2,6-BP, which suppresses glycolytic flux to lactate relative to wild-type control fibroblasts. This glycolytic deficit in turn attenuates anchorage-independent growth in soft agar and the growth and glucose uptake of tumors in mice (21). Based on these observations, small-molecule inhibitors that target the substrate-binding domain of the PFKFB3 isozyme may prove useful as novel antineoplastic agents.

We report herein the identification and characterization of a novel inhibitor of the PFKFB3 isozyme. Using computational modeling and virtual screening of chemical databases, we identified a PFKFB3 isozyme inhibitor, compound 3-(3-pyridinyl)-1-(4-pyridinyl)-2-propen-1-one (3PO), which (*a*) decreases intracellular Fru-2,6-BP and suppresses glycolytic flux in transformed cells; (*b*) is selectively cytostatic to *ras*-transformed cells; (*c*) suppresses tumorigenic growth of breast adenocarcinoma, leukemia, and lung adenocarcinoma cells *in vivo* and; (*d*) reduces Fru-2,6-BP production and $^{18}$F-2-DG uptake by tumors *in situ.* Importantly, the cytostatic effects of 3PO are increased when intracellular Fru-2,6-BP is reduced and suppressed when intracellular Fru-2,6-BP is increased. Taken together, these data provide the first direct evidence that the identification of small-molecule inhibitors of the PFK-2/FBPases may be an important new avenue for the development of novel chemotherapeutic agents.

## Materials and Methods

### PFKFB3 Molecular Modeling and Compound Screen

The PFKFB3 homology model used the X-ray structure of the rat testes PFKFB4 (PDB code 1BIF) isozyme as a structural template. An alignment was generated using Clustal W (22). Four homology models were generated using Modeller (23), and the structure that best reproduced the PFKFB3 binding site (14, 24) was selected for further use. The residues essential to ligand binding and protein activity for PFKFB3 (14, 24) were correlated to equivalent residue numbers in the consensus structure. The model was read into InsightII (Accelrys), and three of the essential residues, $Arg^{66}$, $Tyr^{161}$, and $Thr^{94}$, were selected as the centroid target for the virtual screening runs. We used the Ludi (Accelrys) virtual screening program to process the ChemNavigator iResearch Library (ChemNavigator).[4] After these screening runs were completed, molecules scoring above 500 using Ludi's scoring system were

[4] http://www.chemnavigator.com

analyzed by visual inspection in the active site of the protein. Ligands that were docked correctly in the active pocket were catalogued according to the target and library used for screening. The highest scoring 200 molecules were identified for purchase using Scifinder Scholar and the top 45 were selected for potential experimental assays. All computational work and virtual screening was done in the James Graham Brown Cancer Center Molecular Modeling Facility using a 32-processor SGI Origin 2000 server. The 13 compounds listed below were commercially purchased and examined for inhibitory effects on both Jurkat T cell proliferation and recombinant PFKFB3 activity.

2-(bromo-phenyl)-6-methyl-quinoline-4-carboxylic acid.
2-(bromo-phenyl)-quinoline-4-carboxylic acid.
3-quinolinecarboxaldehyde, 7-methyl-2-(1-piperidinyl).
3PO.
2-chloro-5-(5-formyl-2-furyl) benzoic.
6-chlorobenzimidazole-4-carboxylic acid.
2-chloro-benzylidene-(4-(4-chloro-phenyl)-piperazin-1-yl)-amine.
2-chloro-5-nitro-3-picoline.
3-quinolinecarboxaldehyde, 6-methyl-2-(1-piperidinyl).
(4-chloro-3-nitrophenyl)(1,2,3,6-tetrahydropyridin-1-yl) Methanone.
6-chloro-1-methoxy-2-phenyl-1H-1,3-benzimidazole.
1-(3-bromophenyl)-2-nitropropene.
2,5-diiodo-4-methyl-3-(2-nitrovinyl)pyrrole.

### PFKFB3 Cloning, Expression, and Purification

Human PFKFB3 cDNA was amplified from a preexisting mammalian expression plasmid, and the PCR product was subcloned into the pET-30b(+) vector (Novagen). The pET-30b(+)-PFKFB3C-termHis plasmid was subsequently transformed into BL21 (DE3) *Escherichia coli* competent cells (Novagen). For expression and purification of PFKFB3, a 1 L culture of BL21-PFKFB3 transformed cells was shaken for 16 h at 37°C. After 16 h, an additional 1 L Luria-Bertani medium containing 2 mmol/L isopropyl-β-D-thiogalactopyranoside (final concentration, 1 mmol/L) was added to the culture and shaken for 4 h at 30°C. Bacteria were collected by centrifugation, and protein purification was done as described in the Qiaexpressionist protocol under native conditions (Qiagen). For further purification, elution fractions were dialyzed against a 20 mmol/L Tris-HCl, 200 mmol/L NaCl (pH 7.4) buffer and subjected to gel filtration via Sephadex S200 columns (Amersham).

### PFKFB3 Enzymatic Assays

PFKFB3 protein activity was measured by an enzyme-coupled kinetics assay incorporating pyruvate kinase and lactate dehydrogenase as described previously (25). Control reactions for 3PO inhibition contained increasing amounts of 3PO without addition of PFKFB3. The enzyme kinetics module for SigmaPlot 9.0 was used to calculate the kinetic variables for PFKFB3 and 3PO inhibition ($V_{max}$, $K_m$, and $K_i$). The data represented are the mean ± SD from triplicate measurements from two independent experiments.

### Generation of FLAG-PFKFB3 Construct for Mammalian Expression

FLAG-PFKFB3 containing the complete PFKFB3 coding sequence and FLAG epitope at its $NH_2$ terminus was subcloned into the *Bam*HI/*Hin*dIII restriction sites within the retroviral Tet response vector pRevTRE (Clontech). Recombinant retrovirus was produced by Lipofectamine-mediated (Invitrogen) transfection of the pRevTRE-FLAG-PFKFB3 construct into PT67 packaging cell lines. To create Jurkat cell lines that have stably integrated and express inducible FLAG-PFKFB3, the cells were infected with recombinant retrovirus containing FLAG-PFKFB3, and stable clones were selected in the presence of 400 μg/mL hygromycin (Clontech).

### Cell Culture

The K562, HL-60, MDA-MB231, and melanoma (CRL-11174) human cancer cell lines were purchased from American Type Culture Collection. HeLa, Lewis lung carcinoma, MDA-MB231, melanoma, and PFKFB3$^{+/+}$ or PFKFB3$^{+/-}$ fibroblast cells (21) were grown in DMEM (Hyclone) supplemented with 10% fetal bovine serum (Hyclone) and 50 μg/mL gentamicin sulfate (Invitrogen). The HL-60, K562, and Jurkat cell lines were grown in RPMI 1640 (Hyclone) supplemented with 10% fetal bovine serum and 50 μg/mL gentamicin sulfate. The Jurkat FLAG-PFKFB3 cell line was propagated in RPMI 1640 supplemented with 10% fetal bovine serum, 50 μg/mL gentamicin sulfate, and 400 μg/mL hygromycin. The primary NHBE and the NHBE-hT/LT/*ras* cells were cultured in bronchial epithelial growth medium (Cambrex) with supplements described previously (21). All cell lines were maintained at 5% $CO_2$ at 37°C.

### Cell Cycle Analysis and Flow Cytometry

Jurkat cells were plated at $1 \times 10^5$/mL in RPMI 1640 supplemented with 10% fetal bovine serum and 50 μg/mL gentamicin sulfate. Cells were immediately treated with vehicle or 10 μmol/L 3PO for 0, 4, 8, 16, 24, or 36 h. Cell cycle analysis was done according to the manufacturer's protocol using Vybrant DyeCycle Orange stain (Molecular Probes/Invitrogen). The flow cytometric analysis was done by the flow cytometry laboratory within the Tumor Immunology Program at the University of Louisville James Graham Brown Cancer Center.

### Fru-2,6-BP and Lactate Measurements

Jurkat cells were plated at $1 \times 10^5$/mL and immediately incubated with 10 μmol/L 3PO for 0, 4, 8, 16, 24, or 36 h. Media samples were collected and lactate levels were measured using a lactate oxidase-based colorimetric assay read at 540 nm according to the manufacturer's instructions (Trinity) and normalized to protein concentration. Fru-2,6-BP assays were done as described previously (26).

### 2-Deoxyglucose Uptake

Jurkat cells were plated at $1 \times 10^5$/mL in RPMI 1640 supplemented with 10% fetal bovine serum and 50 μg/mL gentamicin sulfate. Cells were immediately treated with vehicle or 10 μmol/L 3PO for the indicated time periods and subsequently placed in glucose-free RPMI 1640 for 30 min. $^{14}$C-2-deoxyglucose (0.25 μCi/mL; Perkin Elmer)

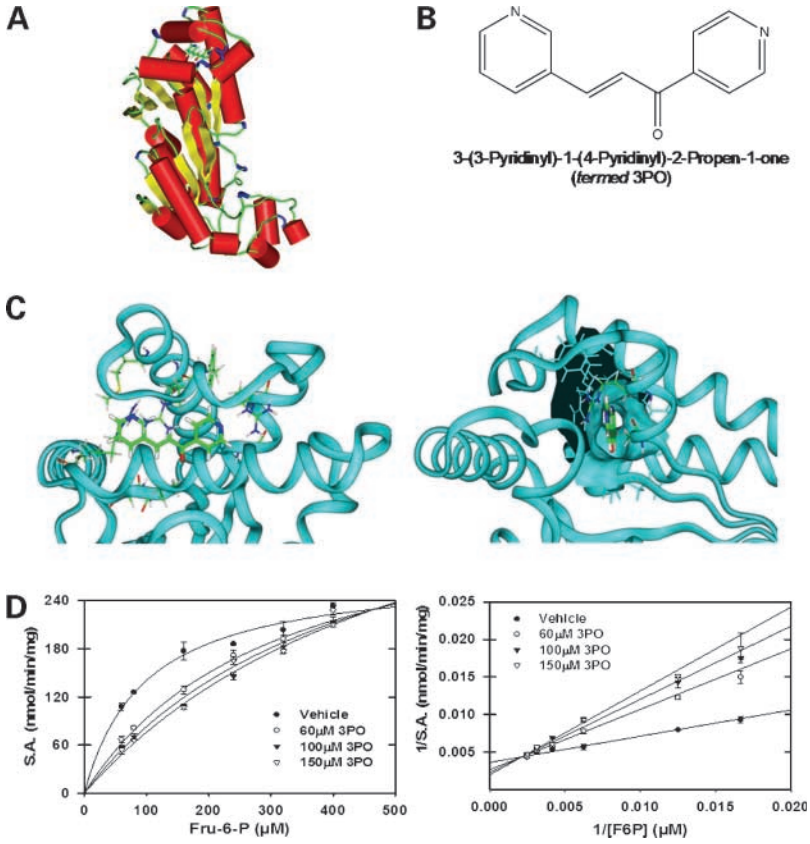


**Figure 2.** Compound 3PO inhibits recombinant PFKFB3 enzyme activity. **A,** homology model of PFKFB3 as determined by molecular modeling. The model is illustrated in secondary structure with 3PO in its respective binding site (*rods*). **B,** molecular structure of 3PO (MW, 210 kDa). **C,** side and end views of the PFKFB3 binding pocket showing residues that are within 2.5Å. 3PO is shown in thicker stick representation than the surrounding protein residues. The fold of PFKFB3 is shown as a cyan ribbon. **D,** *in vitro* recombinant enzyme assays using purified PFKFB3 were done as described in Materials and Methods. Shown are Michaelis-Menten and Lineweaver-Burke double reciprocal plots examining PFKFB3 enzyme activity as a function of Fru-6-P concentration (60, 80, 160, 240, 320, and 400 μmol/L). Kinase assays were done in the presence or absence of 60, 100, and 150 μmol/L 3PO. Mean ± SD of three independent experiments.

was added for an additional 60 min and cells were then washed three with ice-cold RPMI 1640 containing no glucose. Cell lysates were collected in 500 μL of 0.1% SDS, and scintillation counts (counts/min) were measured on 400 μL of lysate. Counts were normalized to protein concentration, and data are represented as mean ± SD from duplicate measurements from two independent experiments.

### Whole-Cell ATP, $NAD^+$, and NADH Determination

Jurkat cells were plated at $1 \times 10^5$/mL and immediately incubated with 10 μmol/L 3PO for the indicated time periods. ATP levels were determined using the ATP determination kit according to the manufacture's protocol (Molecular Probes/Invitrogen) and $NAD^+$ and NADH levels were measured using the EnzyChrom $NAD^+$/NADH assay kit (BioAssay Systems) on $1 \times 10^6$ cells for both vehicle and 3PO-treated samples at all time points.

### Metabolite Extraction for Nuclear Magnetic Resonance

Jurkat cells were treated with vehicle or 10 μmol/L 3PO in the presence of $^{13}$C-glucose for 36 h. The cells were counted and equal numbers of cells were pelleted, washed twice with cold PBS to remove adhering medium, and flash frozen in liquid $N_2$. The cold pellet was extracted with 10% ice-cold trichloroacetic acid (twice) followed by lyophilization. Dry extract was redissolved in 0.35 mL $D_2O$ and loaded into a 5 mm Shigemi tube.

### Nuclear Magnetic Resonance

Nuclear magnetic resonance (NMR) spectra were recorded at 14.1 T on Varian Inova NMR spectrometer at 20°C using a 90° excitation pulse. For analyzing the extracts and determining the positional enrichment with $^{13}$C, two-dimensional experiments were used, including TOCSY and HSQC. Metabolites were assigned based on their $^1$H and $^{13}$C chemical shifts and TOCSY connectivity pattern. All metabolites were quantified by integration of the NMR spectra in the TOCSY experiment. The NMR experiments were done by the Structural Biology Program's NMR Core at the University of Louisville James Graham Brown Cancer Center.

### Protein Extraction and Western Blot Analysis

Protein extraction and Western blots were done as described previously (21). Blots were probed for PFKFB3, stripped, and subsequently reprobed for β-actin using anti-PFKFB3 (Abgent) and anti-β-actin (Sigma), respectively.

### *In vitro* 3PO Growth Inhibition

All cell lines were plated at $1 \times 10^5$/mL in the appropriate medium. For suspension cells, 3PO was added immediately to the medium, whereas 3PO treatment was initiated the following day for adherent cell lines. For dose-dependent experiments, 3PO was added in increasing concentrations for 36 h. For time-dependent experiments, 10 μmol/L 3PO was added at time 0, 4, 8, 16, 24, or 36 h. For PFKFB3 overexpression studies, Jurkat cells containing the

FLAG-PFKFB3 expression vector or a control plasmid were induced by addition of doxycycline (1 μg/mL; Clontech) 24 h before 3PO incubation. Cells were then collected 48 h after treatment, and cell number and viability were determined by trypan blue exclusion. $IC_{50}$s were calculated as the 3PO concentration needed for 50% of vehicle-treated cell growth. The data represented are the mean ± SD from triplicate measurements from three independent experiments.

### *In vivo* Studies

Exponentially growing MDA-MB231 and HL-60 cells were collected, washed, and resuspended in PBS at 20 × $10^7$/mL. Cells were then mixed 1:1 with Matrigel (BD Biosciences), and 0.1 mL of the cell suspension was injected s.c. (1 × $10^7$ cells) into female BALB/c nude mice (20 g). Exponentially growing Lewis lung carcinoma cells were collected, washed twice, and resuspended in PBS (1 × $10^7$/mL). C57Bl/6 female mice (20 g) were injected s.c. with 0.1 mL of the suspension. Body weight and tumor growth were monitored daily throughout the study. Tumor masses were determined by measurement with Vernier calipers using the formula: mass (mg) = [width$^2$ (mm) × length (mm)] / 2 (27). Mice with established tumors (between 130 and 190 mg) were randomized into

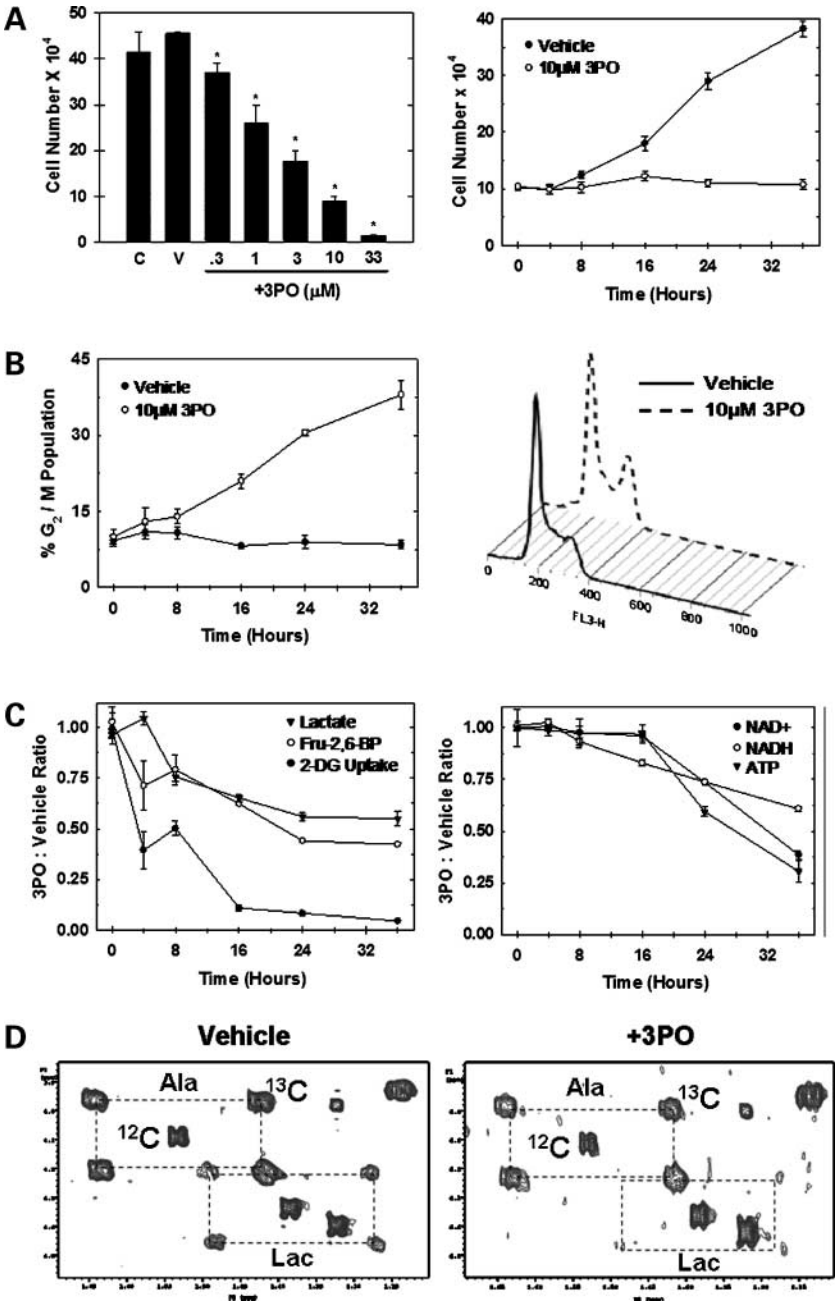


**Figure 3.** 3PO causes $G_2$-M phase arrest, which is preceded by decreased Fru-2,6-BP and glucose uptake. Growth inhibition, Fru-2,6-BP, 2-DG uptake, lactate, ATP, $NAD^+$, NADH, cell cycle, and $^{13}C$-glucose incorporation measurements were done as described in Materials and Methods. Mean ± SD of 3PO/vehicle ratio, unless otherwise specified, of triplicate values from three independent experiments. **A,** dose- and time-dependent effects of 3PO on Jurkat cell (1 × $10^4$ cells in 100 μL) proliferation. Mean ± SD of triplicate values from three independent experiments. $P < 0.001$. **B,** % $G_2$-M cell cycle population of Jurkat cells over time treated with vehicle or 10 μmol/L 3PO. Representative cell cycle histogram as measured by flow cytometry from Jurkat cells treated with vehicle or 10 μmol/L 3PO for 36 h. **C,** lactate secretion, 2-DG uptake, Fru-2,6-BP production, and whole-cell $NAD^+$, NADH, and ATP levels as a function of time in the presence or absence of 10 μmol/L 3PO. **D,** two-dimensional NMR spectra illustrating $^{13}C$ incorporation into alanine (*Ala*) and intracellular lactate (*Lac*) within Jurkat cells after 10 μmol/L 3PO treatment for 36 h. Representative spectrum from three independent experiments. Edge of dashed line boxes correspond to $^{13}C$ peaks for respective metabolites, which are surrounding the endogenous $^{12}C$ peak in the center.

vehicle control or 3PO-treated groups. Vehicle control groups received i.p. injections of 50 μL DMSO, whereas treated groups received 0.07 mg/g 3PO in 50 μL DMSO at the indicated time points. All tumor experiments were conducted three times and the data presented are from one experiment. All protocols were approved by the University of Louisville Institutional Animal Care and Use Committee.

### *In vivo* Fru-2,6-BP Measurement

C57Bl/6 female mice (20 g) were injected s.c. with $1 \times 10^6$ Lewis lung carcinoma cells. When xenografts were measured to have a mass of 150 to 180 mg, mice were randomized and given i.p. injections of vehicle DMSO or 0.07 mg/g 3PO. Four hours after injection, tumors were removed and homogenized in 1 volume of 0.05 mol/L NaOH and subsequently mixed with 1 volume of 0.1 mol/L NaOH. Fru-2,6-BP assays were done as described previously (26).

### Micro-Positron Emission Tomography

Lewis lung carcinoma xenograft-bearing mice were given i.p. injections of 50 μL DMSO or 0.07 mg/g 3PO in DMSO. After 30 min, mice were injected i.p. with $^{18}$F-2-DG (150 μCi, 100 μL in $H_2O$) and subsequently anesthetized after 15 min with 2% isoflurane in oxygen. The mice were then transferred to a R-4 Rodent Scanner micro-positron emission tomography (CTI Concorde Microsystems; $n = 3$).

### Echocardiography

Echocardiograms were done by the University of Louisville Institute of Molecular Cardiology as described previously (28).

### Statistics

Statistical significance for the growth inhibition and *in vivo* studies between control and 3PO treatment was determined by a two-sample, nonparametric, two-tailed $t$ test using Graph Pad Prism version 3.0 (Graph Pad Software). $P < 0.05$ was considered to be statistically significant, and actual $P$ values are shown with corresponding results.

## Results

### Homology Modeling of the PFKFB3 Protein and Virtual Screening for Small-Molecule Inhibitors of PFKFB3 Activity

We generated a homology model of the PFKFB3 isozyme to obtain structural information regarding the fructose-6-phosphate (Fru-6-P) binding sites. The computational model was developed using the X-ray structure of the rat testes PFKFB4 isozyme as the input homologue sequence and structural template. Figure 2A illustrates the final PFKFB3 structural model with particular attention to the residues involved in 3PO binding. The ChemNavigator iResearch Library then was screened for potential PFKFB3 binding compounds using the docking program Ludi and 45 compounds that have the potential to bind the Fru-6-P binding site were identified, scored, and ranked based on their interacting potential.

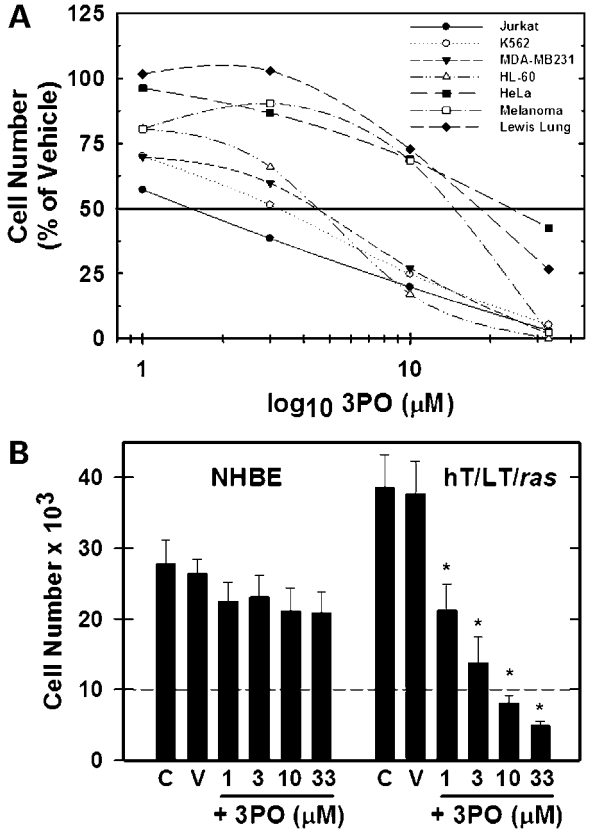


**Figure 4.** Compound 3PO selectively suppresses cellular proliferation of transformed cells. Growth inhibition studies were done as described in Materials and Methods. Mean ± SD of triplicate values from a representative experiment, which was repeated thrice. **A,** inhibition of cellular proliferation of transformed tumor cell lines. Data are % cell growth of vehicle control as $\log_{10}$ of 3PO concentration. **B,** NHBE cells were sequentially immortalized with human telomerase (*ht*) and large T antigen (*LT*) and transformed with oncogenic H-*ras*$^{V12}$. Growth inhibition between primary and transformed NHBE (ht/LT/*ras*) cells treated with increasing concentrations of 3PO. *, $P < 0.01$.

### Small-Molecule Inhibition of Recombinant PFKFB3

We examined the 13 best-score compounds for their ability to inhibit recombinant PFKFB3 isozyme activity and identified a single compound, 3PO, which suppresses the basal enzymatic activity of the PFKFB3 isozyme (Fig. 2B-D). Compound 3PO causes a dose-dependent decrease in the PFK-2 activity of the PFKFB3 isozyme at low concentrations of Fru-6-P, which is overcome by Fru-6-P, suggesting competition between 3PO and Fru-6-P for the PFKFB3 protein binding site (Fig. 2D). However, Lineweaver-Burke double reciprocal plot analyses of the effects of 3PO on PFK-2 activity show that 3PO inhibits through a mixed inhibition mechanism, both competitive and uncompetitive inhibition (Fig. 2D). The specific PFK-2 activity of the recombinant PFKFB3 protein is 277 ± 9 nmol Fru-6-P × $min^{-1}$ × $mg^{-1}$, the $K_m$ for Fru-6-P is 97 μmol/L, and the $K_i$ for 3PO inhibition is 25 ± 9 μmol/L. Importantly, 3PO does not inhibit purified PFK-1 activity (data not shown). These studies confirm that 3PO is an inhibitor of the PFKFB3

isozyme primarily through competition with Fru-6-P and that computational targeting of the PFKFB3 substrate binding site for competitive inhibitors is a valid method for the identification of small-molecule inhibitors of PFK-2/FBPases.

### 3PO Causes $G_2$-M Phase Arrest, Which Is Preceded by Decreased Fru-2,6-BP and Glucose Uptake

We examined the effects of compound 3PO on the proliferation of Jurkat T cell leukemia cells and found that as little as 0.3 μmol/L 3PO caused a decrease in cell proliferation and that 10 μmol/L 3PO completely inhibited proliferation over 36 h (Fig. 3A). The suppression of cell proliferation was the result of a $G_2$-M phase cell cycle arrest as determined by propidium iodide staining (Fig. 3B). We next inspected the effects of 10 μmol/L 3PO on Fru-2,6-BP, 2-deoxyglucose (2-DG) uptake, and lactate secretion and found that 2-DG uptake and Fru-2,6-BP were markedly reduced within 4 h of exposure (Fig. 3C). These metabolic changes were followed by a decrease in lactate secretion (Fig. 3C; 8 h), NADH (Fig. 3C; 16 h), $NAD^+$ (Fig. 3C; 24 h), and ATP (Fig. 3C; 24 h). We then confirmed that direct glycolytic flux to lactate was suppressed by pulsing the Jurkat cells with fully labeled $^{13}$C-glucose during 10 μmol/L 3PO exposure and examining the fate of the $^{13}$C atoms by NMR spectroscopy (Fig. 3D).

### Cytostatic and Cytotoxic Effects of Compound 3PO

We measured the growth and survival of several transformed cells in the presence of vehicle or 3PO and found that all examined solid tumor and hematologic cell lines were sensitive to the cytostatic effects of 3PO (Fig. 4A; $IC_{50}$, 1.4-24 μmol/L). We also examined the effects of 3PO on the growth of primary NHBE cells and NHBE cells that have been immortalized and transformed with telomerase (hT), large T antigen (LT), and H-*ras*$^{V12}$ (hT/LT/*ras* cells; ref. 21) and found that hT/LT/*ras* cells are more sensitive to 3PO (Fig. 4B). We speculate that this increased sensitivity may be due partly to the low steady-state intracellular concentration of Fru-2,6-BP in hT/LT/*ras* cells (2.1 ± 0.6 pmol/mg protein) relative to NHBE cells (11.3 ± 1.6 pmol/mg protein). The low intracellular Fru-2,6-BP coupled with an increased need for high PFK-1 flux may cause *ras*-transformed cells to be particularly sensitive to the PFKFB3 inhibitory properties of 3PO.

### Reduced Intracellular Fru-2,6-BP Sensitizes Cells to Compound 3PO

To examine the role of the PFK-2/FBPases as potential targets of 3PO, we manipulated the protein expression of the PFKFB3 isozyme and then examined the effect on the antigrowth properties of 3PO. If the PFK-2/FBPases are the authentic targets of 3PO, then cells that are genetically manipulated to express decreased PFKFB3 and thus less Fru-2,6-BP should be more sensitive to compound 3PO. As shown in Fig. 5A, PFKFB3$^{+/-}$ LT/*ras*-transformed fibroblasts express decreased PFKFB3 protein and low intracellular Fru-2,6-BP compared with their wild-type genetic matched counterparts (PFKFB3$^{+/+}$ LT/*ras*; Fru-2,6-BP: PFKFB3$^{+/+}$, 60.3 ± 3.7 pmol/mg; PFKFB3$^{+/-}$, 10.3 ± 1.5 pmol/mg; ref. 21). We incubated both cell types with several concentrations of compound 3PO and examined the effects on proliferation. The PFKFB3$^{+/-}$ fibroblasts were more sensitive to compound 3PO treatment ($IC_{50}$, 26 μmol/L) compared with the wild-type PFKFB3$^{+/+}$ transformed cells ($IC_{50}$, 49 μmol/L; Fig. 5B).

### Ectopic Expression of PFKFB3 in Jurkat T Cell Leukemia Cells Confers 3PO Resistance

If compound 3PO slows growth through inhibition of PFK-2 activity, then ectopic expression of the PFKFB3 isozyme may thwart the cytostatic activity of 3PO. We used the Tet-On two-vector system to transiently induce PFKFB3 protein expression with doxycycline and then exposed the cells to 3PO. We found that doxycycline-induced ectopic expression of PFKFB3 protein increased intracellular

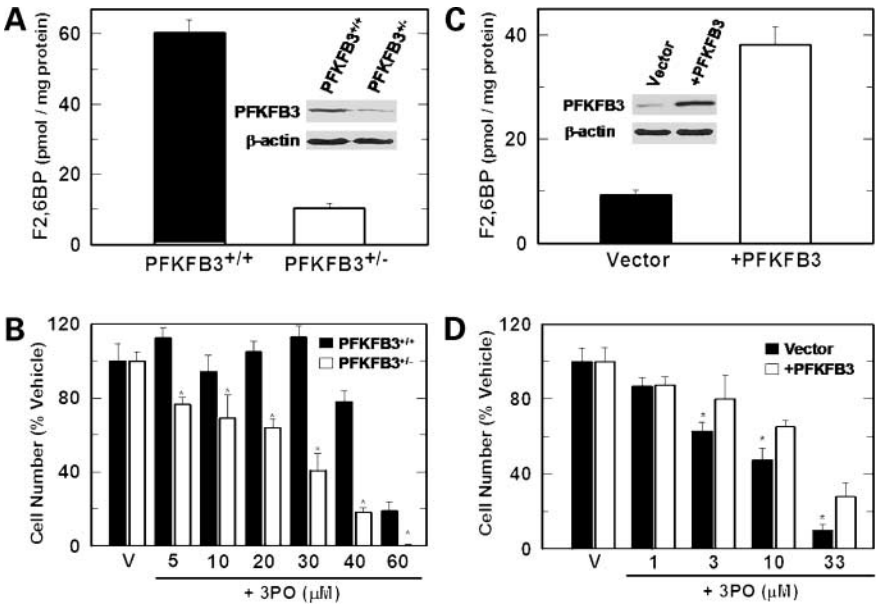


**Figure 5.** Compound 3PO targets PFKFB3 *in situ*. F2,6BP measurements, Western blot analysis, and the antiproliferative effects of 3PO incubation were determined as described in Materials and Methods. **A** and **B,** fibroblasts from wild-type (+/+) or haploinsufficient (+/–) PFKFB3 mice were immortalized with large T antigen (*LT*) and transformed with oncogenic H-*ras*$^{V12}$. **C** and **D,** Jurkat cells were engineered to overexpress PFKFB3 after doxycycline treatment with a Tet-On system. **A** and **C,** cellular levels of Fru-2,6-BP and PFKFB3 expression (*inset*). **B** and **D,** cells were incubated with the indicated concentrations of 3PO, and viable cells were counted after 48 h. For Jurkat cells, 24 h before 3PO treatment, 1 μg/mL doxycycline was added to induce PFKFB3 protein levels. Control cells containing an empty vector were similarly treated with doxycycline and served as background PFKFB3 expression. Mean ± SD of triplicate values from a representative experiment. *, $P < 0.01$, statistical difference between vehicle control and 3PO-treated samples.

Fru-2,6-BP (Fig. 5C; vector control, 9.2 ± 0.95 pmol/mg; +PFKFB3, 38.1 ± 3.4 pmol/mg) and protected the Jurkat cells from the cytostatic effects of 3PO (Fig. 5D; vector alone, $IC_{50}$, 8.9 μmol/L; +PFKFB3, $IC_{50}$, 19.3 μmol/L). The coupled observations that genomic deletion of *PFKFB3* sensitizes cells to compound 3PO and ectopic expression of the PFKFB3 isozyme confers resistance to 3PO substantially support the targeting of intracellular PFK-2 activity as the mechanism of action of 3PO.

### Compound 3PO Administration Inhibits the Growth of Established Tumors in Mice

To investigate the ability of compound 3PO to suppress tumor growth *in vivo*, we conducted a dose escalation toxicity trial in C57Bl/6 mice and found that an i.p. dose of 0.07 mg/g daily was well tolerated and caused no adverse effects. We selected three xenograft models of tumorigenesis: (*a*) Lewis lung carcinoma in C57Bl/6 mice, (*b*) MDA-MB231 breast adenocarcinoma cells in athymic mice, and (*c*) HL-60 promyelocytic leukemia cells in athymic mice. We chose to examine the efficacy of compound 3PO against established tumors as opposed to the initial outgrowth of injected transformed cells, because we anticipate that phase I clinical trials will be conducted in patients with established tumors rather than in the adjuvant setting. In the first tumor model, C57Bl/6 mice bearing established Lewis lung carcinomas were given i.p. injections of either DMSO or 0.07 mg/g 3PO in DMSO once daily for 14 days. Compound 3PO significantly suppressed the growth of Lewis lung carcinoma xenografts compared with the DMSO control group (Fig. 6A). In the second model, MDA-MB231 human breast adenocarcinoma tumors were established in BALB/c athymic mice and the administration frequency was reduced to a cyclic regimen of three daily doses followed by 3 days of no drug administration. Surprisingly, we observed total inhibition of xenograft tumorigenic growth of MDA-MB231 cells compared with the DMSO controls (Fig. 6B). The third model of tumorigenesis consisted of HL-60 leukemia cell xenografts established in BALB/c athymic mice. In this model, we further reduced the treatment schedule to a regimen of two daily injections followed by 7 consecutive days of no injections. As shown in Fig. 6C, 3PO treatment given daily twice every 9 days significantly inhibited HL-60 tumor growth. Interestingly, the efficacy of the second administration cycle is easily appreciated by the reduction in growth seen after treatment on day 9. Taken together, these data indicate that selective suppression of intracellular PFK-2 activity may prove useful as an antineoplastic strategy.

### Compound 3PO Decreases Fru-2,6-BP and Glucose Uptake *In vivo*

We examined the Fru-2,6-BP concentration in established xenografts after i.p. injection of vehicle DMSO or 0.07 mg/g 3PO. Compound 3PO treatment significantly reduced Fru-2,6-BP in tumor xenografts *in vivo* compared with vehicle control (vehicle: 13.1 ± 1.9 pmol/mg, 3PO: 8.5 ± 1.7 pmol/mg). To investigate the effect of 3PO treatment on glucose uptake, we conducted micro-positron emission tomography analysis on xenograft-bearing mice after

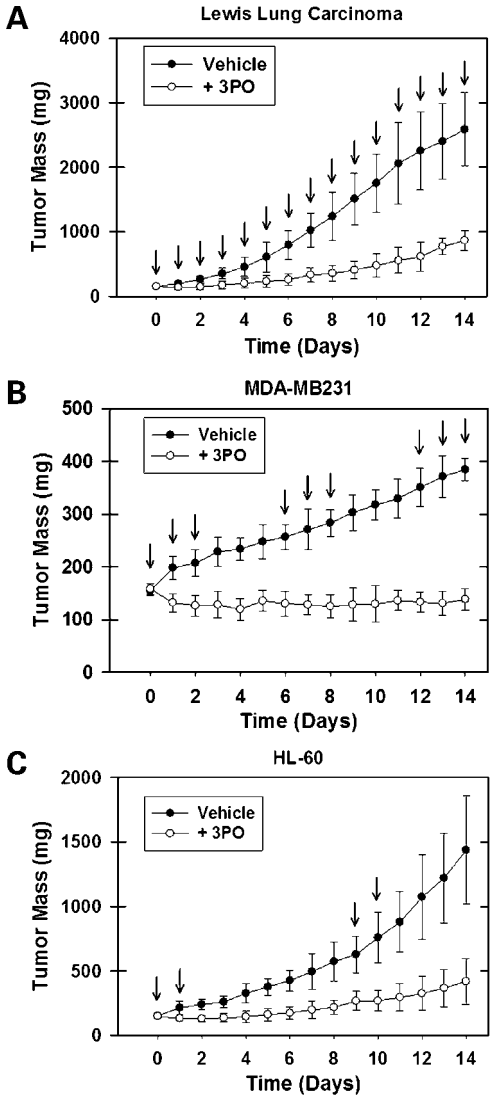


**Figure 6.** Compound 3PO administration suppresses growth of tumor xenografts *in vivo*. Lewis lung carcinoma, MDA-MB231, and HL-60 xenografts were initiated as described in Materials and Methods. Tumors were measured daily using blunt-end Vernier calipers, and mice with established tumors (130-190 mg) were blindly randomized into either DMSO control (*filled circles*) or 3PO treatment (*open circles*) groups. Experimental mice were weighed and given i.p. injections of either 50 μL DMSO or 0.07 mg/g 3PO in 50 μL DMSO at the indicated time points. *Arrows,* control or 3PO daily administrations. Each tumor experiment was repeated three times. Data are from one experiment for each animal model of tumorigenesis. **A,** Lewis lung carcinoma xenografts were established in C57Bl/6 mice. Experimental mice were given repeated daily injections of DMSO ($n$ = 11) or 3PO ($n$ = 14) for the entire duration of the study (14 d). $P < 0.0003$, statistically significant difference between DMSO and 3PO groups obtained after initial injection (*Day 2*). **B,** BALB/c athymic mice with established MDA-MB231 breast adenocarcinoma xenografts were given a cyclical dosing regiment of three sequential daily injections of either DMSO or 3PO followed by 3 off days for the duration of the study (14 d). $P < 0.0001$, statistical difference between the DMSO control ($n$ = 14) and 3PO experimental ($n$ = 13) groups observed on day 2. **C,** HL-60 acute promyelocytic leukemia xenografts were established in BALB/c athymic mice. Mice were given a cyclical regimen of two daily injections of DMSO or 3PO with a subsequent 7-d rest period for a total of 14 d. $P < 0.0001$, statistical difference obtained after initial injection between DMSO ($n$ = 11) and 3PO ($n$ = 12) treatment groups.

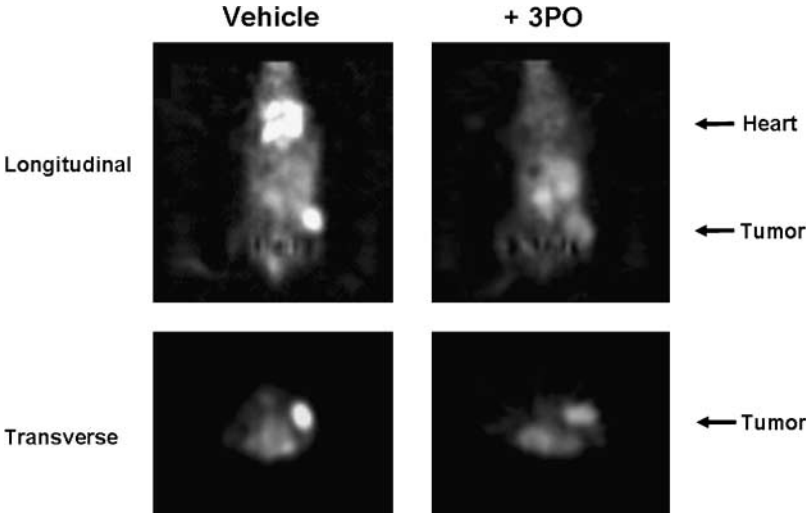


**Figure 7.** Compound 3PO treatment reduces *in situ* glucose uptake in tumor xenografts. $^{18}$F-2-DG uptake in mice bearing Lewis lung carcinoma xenografts were analyzed as described in Materials and Methods. The procedures were done on three sets of animals with similar tumor masses (150-180 mg) treated with DMSO or 0.07 mg/g 3PO. Micro-positron emission tomography images of $^{18}$F-2DG uptake within a representative mouse pair. *Arrows,* position of the heart and the tumor xenograft within the right flank of a single animal pre- and post-administration of 3PO.

administration of either vehicle or 0.07 mg/g 3PO. As illustrated in Fig. 7, 3PO treatment diminished $^{18}$F-2-DG uptake within the xenograft compared with the DMSO-treated mouse. We also observed a difference in cardiac $^{18}$F-2-DG uptake between the treated and the untreated mice and speculated that targeting of PFK-2/FBPases may prove to be cardiotoxic. However, echocardiographic examination of cardiac function revealed no acute changes in ejection fraction (DMSO: 69 $\pm$ 4%, +3PO: 71 $\pm$ 6%).

## Discussion

Pharmacologic disruption of glycolysis has emerged as a novel antineoplastic strategy due to the observations that tumor cells metabolize glucose more rapidly than adjacent normal cells and are more sensitive to glucose deprivation (29). 3-Bromopyruvate and 2-DG are two well-studied examples of compounds that inhibit the first irreversible enzyme of glycolysis, hexokinase, and suppress tumor growth *in vivo* (30–32). Interestingly, several recently developed chemotherapeutic agents that target oncogene protein products have been found to function in part by suppressing the glucose metabolism of transformed cells. For example, the BCR/ABL inhibitor Imatinib (Gleevec) and farnesyl transferase inhibitors that disrupt *ras* signaling both depress glycolysis at doses below that required for cell death (6, 33). Taken together, these observations support the clinical development of antiglycolytic agents as novel chemotherapeutic agents.

Although PFK-1 is the second irreversible enzyme in glycolysis and is increased in neoplastic tissues and transformed cells (10, 34, 35), PFK-1 inhibitors that suppress tumor growth have not yet been identified. PFK-1 activity is dependent on the intracellular concentration of Fru-2,6-BP generated by the PFK-2/FBPase family of enzymes (encoded by the genes *PFKFB1-4*) and neoplastic cells may be especially sensitive to PFK-2 inhibition given their need for increased glycolysis. In this report, we describe the identification and initial characterization of the first small-molecule inhibitor of the inducible PFK-2/FBPase isozyme (PFKFB3) that not only is selectively cytostatic to transformed cells ($IC_{50}$, 1.4-24 μmol/L) but also suppresses the growth of three established tumor types in mice. Although optimization of the 3PO structure will likely lead to more active derivatives, several successful chemotherapies display surprisingly high median $IC_{50}$s for cancer cells [e.g., paclitaxel mean $IC_{50}$ 23 μmol/L in 28 lung cancer cell lines (36), cyclophosphamide $IC_{50}$ 10.0 mmol/L in MCF-7 breast adenocarcinoma cells (37), and oxaloplatin mean $IC_{50}$ 4 μmol/L in two colon adenocarcinoma cell lines (38)]. Accordingly, compound 3PO has cytostatic activities that are within the realm of the activities of preexisting chemotherapeutic agents currently in widespread use.

The observations that 3PO decreases intracellular Fru-2,6-BP, 2-DG uptake, and lactate secretion before $G_2$-M phase arrest provide substantial corollary support for the hypothesis that 3PO inhibits cellular proliferation through disruption of energetic and anabolic metabolism. The $G_2$-M arrest caused by 3PO may be secondary to the high requirement for ATP during the $G_2$-M phase of the cell cycle as has been observed previously in HL-60 promyelocytic leukemia cells (39). NMR spectroscopic tracking of $^{13}$C-glucose revealed suppression of glycolytic flux into lactate but not alanine. Alanine and lactate share the same pyruvate pool, but glucose-derived lactate production may be especially affected by inhibition of glycolysis because lactate dehydrogenase requires a ready supply of NADH, a product of glycolytic flux through glyceraldehyde-3-phosphate dehydrogenase. In previous studies, we showed that heterozygotic genomic deletion of the molecular target of 3PO, PFKFB3, specifically inhibits both glycolysis and anchorage-independent spheroid growth of *ras*-transformed lung fibroblasts (21). Based on these studies, we speculate that transformed cells may be distinctly sensitive to inhibition of glycolytic flux when oxygen and glucose diffusion limitations are caused by surrounding cells in

three-dimensional masses. Importantly, increased glycolysis is essential for neoplastic survival and growth and we anticipate that 3PO may yield synergistic antineoplastic effects in combination with other chemotherapeutic agents and/or ionizing irradiation.

Although compound 3PO does not directly inhibit recombinant PFK-1 activity, we have not ruled out the possibility that 3PO may be inhibiting several of the PFK-2/FBPase isozymes simultaneously. Most transformed cells coexpress the PFKFB2-4 protein products at different ratios and the cells examined are no exception (ref. 21; data not shown). The substrate-binding domains of the four isozymes are highly homologous, and we anticipate that some degree of crossover inhibition will occur although 3PO was computationally selected to inhibit the PFKFB3 isozyme. Additionally, several other enzymes bind Fru-6-P and thus may be affected by 3PO, including transketolase, transaldolase, and glutamine:-Fru-6-P transferase. However, we did find that heterozygous PFKFB3$^{+/-}$ transformed fibroblasts are more sensitive to 3PO than wild-type control cells and that induction of PFKFB3 protein expression protects Jurkat cells against compound 3PO. We speculate that the decreased Fru-2,6-BP concentration in the PFKFB3$^{+/-}$ cells may sensitize the energy metabolism of the cells to further suppression of PFKFB3 activity as has been postulated for *ras*-transformed cells (21, 40). Regardless, these observations provide direct support for the hypothesis that 3PO inhibits cellular proliferation through suppression of PFKFB3 activity.

Compound 3PO is a novel small-molecule inhibitor of the PFKFB3 isozyme that (*a*) reduces glycolytic flux resulting in cell growth inhibition, (*b*) is selectively cytostatic to transformed cells, and (*c*) inhibits tumorigenic growth *in vivo*. We have presented substantial evidence via genetic manipulations of *PFKFB3* for the importance of PFK-2/FBPase activity as a metabolic target for compound 3PO and we anticipate that these results will support the further development of PFK-2/FBPase inhibitors as antineoplastic agents.

**Acknowledgments**

We thank Otto Grubraw for helpful discussions, Robert Mitchell for providing the ras$^{V12}$ and LT retroviruses, Barrett Rollins for providing the hT/LT/ras bronchial epithelial cells, Richard Bucala for assistance with the development of the PFKFB3$^{+/-}$ mice, the laboratory of Sumanth Prabhu for doing the echocardiography, and the laboratory of Jun Yan for doing the flow cytometry.

**References**

**1.** Wechalekar K, Sharma B, Cook G. PET/CT in oncology—a major advance. Clin Radiol 2005;60:1143 – 55.

**2.** Warburg O. On the origin of cancer cells. Science 1956;123:309 – 14.

**3.** Warburg O, Posener K, Negelein E. On the metabolism of cancer cells. Biochem Z 1924;152:319 – 44.

**4.** Dang CV, Resar LM, Emison E, et al. Function of the c-Myc oncogenic transcription factor. Exp Cell Res 1999;253:63 – 77.

**5.** Osthus RC, Shim H, Kim S, et al. Deregulation of glucose transporter 1 and glycolytic gene expression by c-Myc. J Biol Chem 2000;275: 21797 – 800.

**6.** Blum R, Jacob-Hirsch J, Amariglio N, Rechavi G, Kloog Y. Ras inhibition in glioblastoma down-regulates hypoxia-inducible factor-1α, causing glycolysis shutdown and cell death. Cancer Res 2005;65:999 – 1006.

**7.** Mazurek S, Zwerschke W, Jansen-Durr P, Eigenbrodt E. Metabolic cooperation between different oncogenes during cell transformation: interaction between activated ras and HPV-16 E7. Oncogene 2001;20: 6891 – 8.

**8.** Ramanathan A, Wang C, Schreiber SL. Perturbational profiling of a cell-line model of tumorigenesis by using metabolic measurements. Proc Natl Acad Sci U S A 2005;102:5992 – 7.

**9.** Vizan P, Boros LG, Figueras A, et al. K-ras codon-specific mutations produce distinctive metabolic phenotypes in NIH3T3 mice [corrected] fibroblasts. Cancer Res 2005;65:5512 – 5.

**10.** Kole HK, Resnick RJ, Van Doren M, Racker E. Regulation of 6-phosphofructo-1-kinase activity in ras-transformed rat-1 fibroblasts. Arch Biochem Biophys 1991;286:586 – 90.

**11.** Racker E, Resnick RJ, Feldman R. Glycolysis and methylaminoisobutyrate uptake in rat-1 cells transfected with ras or myc oncogenes. Proc Natl Acad Sci U S A 1985;82:3535 – 8.

**12.** Van Schaftingen E, Jett MF, Hue L, Hers HG. Control of liver 6-phosphofructokinase by fructose 2,6-bisphosphate and other effectors. Proc Natl Acad Sci U S A 1981;78:3483 – 6.

**13.** Okar DA, Lange AJ. Fructose-2,6-bisphosphate and control of carbohydrate metabolism in eukaryotes. Biofactors 1999;10:1 – 14.

**14.** Chesney J, Mitchell R, Benigni F, et al. An inducible gene product for 6-phosphofructo-2-kinase with an AU-rich instability element: role in tumor cell glycolysis and the Warburg effect. Proc Natl Acad Sci U S A 1999;96:3047 – 52.

**15.** Hamilton JA, Callaghan MJ, Sutherland RL, Watts CK. Identification of PRG1, a novel progestin-responsive gene with sequence homology to 6-phosphofructo-2-kinase/fructose-2,6-bisphosphatase. Mol Endocrinol 1997;11:490 – 502.

**16.** Manzano A, Rosa JL, Ventura F, et al. Molecular cloning, expression, and chromosomal localization of a ubiquitously expressed human 6-phosphofructo-2-kinase/fructose-2, 6-bisphosphatase gene (PFKFB3). Cytogenet Cell Genet 1998;83:214 – 7.

**17.** Sakai A, Kato M, Fukasawa M, Ishiguro M, Furuya E, Sakakibara R. Cloning of cDNA encoding for a novel isozyme of fructose 6-phosphate, 2-kinase/fructose 2,6-bisphosphatase from human placenta. J Biochem (Tokyo) 1996;119:506 – 11.

**18.** Minchenko A, Leshchinsky I, Opentanova I, et al. Hypoxia-inducible factor-1-mediated expression of the 6-phosphofructo-2-kinase/fructose-2,6-bisphosphatase-3 (PFKFB3) gene. Its possible role in the Warburg effect. J Biol Chem 2002;277:6183 – 7.

**19.** Atsumi T, Chesney J, Metz C, et al. High expression of inducible 6-phosphofructo-2-kinase/fructose-2,6-bisphosphatase (iPFK-2; PFKFB3) in human cancers. Cancer Res 2002;62:5881 – 7.

**20.** Calvo MN, Bartrons R, Castano E, Perales JC, Navarro-Sabate A, Manzano A. PFKFB3 gene silencing decreases glycolysis, induces cell-cycle delay and inhibits anchorage-independent growth in HeLa cells. FEBS Lett 2006;580:3308 – 14.

**21.** Telang S, Yalcin A, Clem AL, et al. Ras transformation requires metabolic control by 6-phosphofructo-2-kinase. Oncogene 2006;25: 7225 – 34.

**22.** Chenna R, Sugawara H, Koike T, et al. Multiple sequence alignment with the Clustal series of programs. Nucleic Acids Res 2003; 31:3497 – 500.

**23.** Sali A, Blundell TL. Comparative protein modelling by satisfaction of spatial restraints. J Mol Biol 1993;234:779 – 815.

**24.** Bertrand L, Vertommen D, Freeman PM, et al. Mutagenesis of the fructose-6-phosphate-binding site in the 2-kinase domain of 6-phosphofructo-2-kinase/fructose-2,6-bisphosphatase. Eur J Biochem 1998;254: 490 – 6.

**25.** Bucher J, Pfleiderer G. Pyruvate kinase from muscle. Methods Enzymol 1955;1:435 – 40.

**26.** Van Schaftingen E, Lederer B, Bartrons R, Hers HG. A kinetic study of pyrophosphate: fructose-6-phosphate phosphotransferase from potato tubers. Application to a microassay of fructose 2,6-bisphosphate. Eur J Biochem 1982;129:191 – 5.

**27.** Taetle R, Rosen F, Abramson I, Venditti J, Howell S. Use of nude mouse xenografts as preclinical drug screens: *in vivo* activity of established chemotherapeutic agents against melanoma and ovarian carcinoma xenografts. Cancer Treat Rep 1987;71:297 – 304.

**28.** Dawn B, Stein AB, Urbanek K, et al. Cardiac stem cells delivered intravascularly traverse the vessel barrier, regenerate infarcted myocardium,

and improve cardiac function. Proc Natl Acad Sci U S A 2005;102: 3766 – 71.

**29.** Shim H, Chun YS, Lewis BC, Dang CV. A unique glucose-dependent apoptotic pathway induced by c-Myc. Proc Natl Acad Sci U S A 1998;95: 1511 – 6.

**30.** Liu H, Hu YP, Savaraj N, Priebe W, Lampidis TJ. Hypersensitization of tumor cells to glycolytic inhibitors. Biochemistry 2001;40:5542 – 7.

**31.** Maher JC, Krishan A, Lampidis TJ. Greater cell cycle inhibition and cytotoxicity induced by 2-deoxy-D-glucose in tumor cells treated under hypoxic vs aerobic conditions. Cancer Chemother Pharmacol 2004;53: 116 – 22.

**32.** Xu RH, Pelicano H, Zhou Y, et al. Inhibition of glycolysis in cancer cells: a novel strategy to overcome drug resistance associated with mitochondrial respiratory defect and hypoxia. Cancer Res 2005;65: 613 – 21.

**33.** Boren J, Cascante M, Marin S, et al. Gleevec (STI571) influences metabolic enzyme activities and glucose carbon flow toward nucleic acid and fatty acid synthesis in myeloid tumor cells. J Biol Chem 2001;276: 37747 – 53.

**34.** Hennipman A, Smits J, van Oirschot B, et al. Glycolytic enzymes in breast cancer, benign breast disease and normal breast tissue. Tumour Biol 1987;8:251 – 63.

**35.** Sanchez-Martinez C, Aragon JJ. Analysis of phosphofructokinase subunits and isozymes in ascites tumor cells and its original tissue, murine mammary gland. FEBS Lett 1997;409:86 – 90.

**36.** Georgiadis MS, Russell EK, Gazdar AF, Johnson BE. Paclitaxel cytotoxicity against human lung cancer cell lines increases with prolonged exposure durations. Clin Cancer Res 1997;3:449 – 54.

**37.** Chhipa RR, Singh S, Surve SV, Vijayakumar MV, Bhat MK. Doxycycline potentiates antitumor effect of cyclophosphamide in mice. Toxicol Appl Pharmacol 2005;202:268 – 77.

**38.** Raymond E, Buquet-Fagot C, Djelloul S, et al. Antitumor activity of oxaliplatin in combination with 5-fluorouracil and the thymidylate synthase inhibitor AG337 in human colon, breast and ovarian cancers. Anticancer Drugs 1997;8:876 – 85.

**39.** Sweet S, Singh G. Accumulation of human promyelocytic leukemic (HL-60) cells at two energetic cell cycle checkpoints. Cancer Res 1995; 55:5164 – 7.

**40.** Chesney J. 6-Phosphofructo-2-kinase/fructose-2,6-bisphosphatase and tumor cell glycolysis. Curr Opin Clin Nutr Metab Care 2006;9:535 – 9.